Channel Coding Rate for Finite Blocklength Faster-than-Nyquist Signaling

Mostafa Mohammadkarimi, *Member, IEEE*, Robert Schober, *Fellow, IEEE*, and Vincent W. S. Wong, *Fellow, IEEE*

***Abstract*—The fundamental tradeoff between low latency and high reliability makes the design of ultra-reliable low-latency communications (URLLC) wireless systems challenging. To support URLLC for a fixed bandwidth, faster-than-Nyquist (FTN) signaling is a promising approach since it increases the degrees of freedom (i.e., channel uses) per time interval, which can be exploited to improve reliability. In this letter, we derive analytical expressions for the approximate maximum channel coding rate (MCCR) for finite blocklength FTN signaling for water-filling and equal power allocations. We show that for practical non-sinc square-root Nyquist pulses, the penalty on the rate incurred due to the finite blocklength can be significantly reduced by non-orthogonal FTN transmission. Our results reveal that the MCCR for finite blocklength FTN signaling exceeds the Shannon capacity achieved for infinite blocklength and orthogonal transmission.**

***Index Terms*—Faster-than-Nyquist (FTN) signaling, finite blocklength, channel dispersion, constrained channel capacity.**

I. Introduction

Nyquist signaling relies on the orthogonality of pulses to avoid intersymbol interference (ISI), leading to low-complexity receivers. However, for practical non-sinc pulses, the spectral efficiency is reduced in order to preserve such orthogonality. The reduction in spectral efficiency becomes more relevant for short burst transmission, which is widely employed for the low latency communication use case in the fifth generation (5G) wireless systems [1].

Unlike Nyquist signaling, faster-than-Nyquist (FTN) signaling uses non-orthogonal transmission to achieve a higher Shannon information rate for practical non-sinc pulses satisfying Nyquist's symmetry condition, such as square-root raised-cosine (SRRC) pulses. In fact, FTN signaling achieves the capacity upper bound by taking into account the power spectral density (PSD) of the transmit pulse. Spectral efficiency can be improved by up to a factor of two compared to Nyquist signaling for a given transmit energy per bit. The higher spectral efficiency of FTN signaling is attributed to its capability to exploit the excess bandwidth introduced by non-sinc pulses through non-orthogonal transmission [2], [3].

With the advent of ultra-reliable and low-latency communications (URLLC), recent information-theoretic studies have analyzed the achievable rate in the finite blocklength regime [4]–[7]. In particular, it has been shown that when the packets are short, the achievable rate for a given blocklength and maximum block error probability (MBEP) is subject to a penalty compared to Shannon's channel capacity. This penalty is characterized by the channel dispersion and is inversely proportional to the square root of the packet length, i.e., as the packet length decreases, the penalty increases [4].

Since FTN signaling can increase the number of channel uses per time interval, it is attractive for URLLC use cases. In particular, FTN signaling can be employed to mitigate the rate penalty in short packet transmission. However, to the best of the authors' knowledge, the maximum channel coding rate (MCCR) for FTN signaling in the finite blocklength regime has not been studied in the literature, yet.

In this letter, we derive an analytical expression for the MCCR for finite blocklength FTN signaling. We show that for FTN signaling, the channel can be equivalently modeled as a finite number of parallel frequency-nonselective additive white Gaussian noise (AWGN) channels with different signal-to-noise ratios (SNRs). Based on this model, the achievable MCCR for a given blocklength, MBEP, and PSD of the square-root Nyquist pulse shape is derived.

II. Signal Model and Preliminaries

We consider a real-valued[1] bandlimited baseband AWGN channel with one-sided bandwidth B over which short packets of length N are transmitted with FTN signaling. The received signal of a packet is given as follows

$$x(t) = \sum_{m=0}^{N-1} a_m h(t - m\tau T_{\rm s}) + w(t), \tag{1}$$

where a_m is the m-th transmitted real-valued symbol with $\mathbb{E}\{a_m^2\} = p_m$ ($\mathbb{E}\{\cdot\}$ denotes statistical expectation), $\sum_{m=0}^{N-1} p_m = N\sigma_{\rm a}^2$, $h(t)$ is a unit-energy square-root Nyquist pulse with one-sided bandwidth B, $B \in [W, 2W]$, $T_{\rm s} \triangleq 1/(2W)$ is the smallest time shift for which $h(t)$ is orthogonal, τ, $0 < \tau < 1$, is the time-squeezing factor, and $1/(\tau T_{\rm s})$ is the signaling rate. Furthermore, $w(t)$ is AWGN with PSD $N_0/2$. The average received power for FTN signaling is $\sigma_{\rm a}^2/(\tau T_{\rm s})$.

A. Capacity Results for FTN Signaling

Shannon's channel capacity characterizes the maximum rate at which reliable communication is feasible when there is no restriction on the packet length, i.e., $N \to \infty$. The highest transmission rate of the real-valued AWGN channel in (1) for Nyquist signaling (orthogonal transmission), i.e., for $\tau = 1$, is bounded by the Nyquist capacity $C_{\rm N}$ as follows [8]

$$C_{\rm N} = W \log_2\left(1 + \frac{P}{N_0 W}\right), \tag{2}$$

where $P \triangleq 2W\sigma_{\rm a}^2$. Note that the Nyquist capacity in (2) does not depend on the pulse shape since the received symbols after matched filtering and sampling at the Nyquist rate $2W$ are orthogonal.

Orthogonal signaling is optimal only if $h(t)$ is a sinc-pulse with bandwidth $B = W$. For non-sinc pulses, the channel capacity is higher. For independent and identically distributed (i.i.d.) transmission (i.e., $p_m = \sigma_a^2$, $\forall m$), the channel capacity is given as follows [3]

$$C_{\rm FTN}^{\rm IID} = \int_0^B \log_2\left(1 + \frac{2P_{\rm s}|H(f)|^2}{N_0}\right) {\rm d}f, \tag{3}$$

M. Mohammadkarimi and V. W. S. Wong are with the Department of Electrical and Computer Engineering, The University of British Columbia, Vancouver, Canada (e-mail: {mmkarimi, vincentw}@ece.ubc.ca).

R. Schober is with the Institute for Digital Communications, University of Erlangen-Nuremberg, Erlangen, Germany (e-mail: robert.schober@fau.de).

[1]As is customary for capacity and rate analysis [3], [4], we consider a real-valued channel model. The extension to complex channels is straightforward.

where $P_{\rm s} \triangleq PB/W = 2B\sigma_{\rm a}^2$ and $H(f) = \int_{-\infty}^{+\infty} h(t)e^{-j2\pi ft}$ dt denotes the frequency response of $h(t)$. $C_{\rm FTN}^{\rm IID}$ can be achieved by FTN signaling with i.i.d. real-valued Gaussian symbols a_m and time-squeezing factor $\tau = 1/(2BT_{\rm s})$ [3]. Further improvement is possible if non-i.i.d. FTN signaling is employed. In this case, the capacity is given by [9]

$$C_{\rm FTN}^{\rm NIID} = \int_0^B \log_2\left(1 + \frac{4Bp(f)|H(f)|^2}{N_0}\right) {\rm d}f, \tag{4}$$

where $p(f)$ is given by

$$p(f) = \left[\Theta - \frac{N_0}{4B|H(f)|^2}\right]^+, \tag{5}$$

and constant Θ satisfies

$$2\int_0^B \left[\Theta - \frac{N_0}{4B|H(f)|^2}\right]^+ {\rm d}f = P_{\rm s}. \tag{6}$$

Here, $[x]^+ \triangleq \max(0,x)$ and $p(f)$, $|f| < B$, is the water-filling power allocation at frequency f. For practical non-sinc square-root Nyquist pulses, we have $C_{\rm FTN}^{\rm NIID} > C_{\rm FTN}^{\rm IID} > C_{\rm N}$, due to the non-zero excess bandwidth of these pulses. On the other hand, if $h(t)$ is a sinc-pulse with bandwidth $B = W$, we have $C_{\rm FTN}^{\rm NIID} = C_{\rm FTN}^{\rm IID} = C_{\rm N}$.

B. Capacity Results for Finite Blocklength Coding

Recently, it has been shown that for the AWGN channel with Nyquist capacity $C_{\rm N}$, the MCCR $R_{\rm N}(N,\epsilon)$ [bits/s] for a given finite blocklength N and a given MBEP ϵ can be expressed as [4]

$$R_{\rm N}(N,\epsilon) = C_{\rm N} - 2W\sqrt{\frac{V_{\rm N}}{N}}Q^{-1}(\epsilon) + \frac{W\log_2 N}{N} + \mathcal{O}\left(\frac{1}{N}\right), \tag{7}$$

where $V_{\rm N} = \frac{1}{2}(\log_2 e)^2(1 - 1/(1 + P/(WN_0))^2)$ denotes the Nyquist channel dispersion, $Q(x) \triangleq \frac{1}{\sqrt{2\pi}}\int_x^\infty e^{-t^2/2}{\rm d}t$ is the Gaussian Q-function, and $\mathcal{O}(\cdot)$ is the big-O notation. The channel dispersion is defined as the variance of the information density under the capacity achieving distribution. We note that the classical Nyquist channel capacity is obtained from (7) as $C_{\rm N} = \lim_{N\to\infty}\lim_{\epsilon\to 0} R_{\rm N}(N,\epsilon)$. In the next section, in analogy to (7), we extend (3) and (4) to the finite blocklength regime.

III. Finite Blocklength FTN Signaling

In this section, we first model the continuous-time AWGN channel for FTN signaling equivalently by a finite number of parallel discrete-time AWGN channels. Based on this representation, we then derive the MCCRs for FTN signaling for both i.i.d. and non-i.i.d. transmission in terms of the channel dispersion of parallel AWGN channels. Then, by exploiting Szegö's theorem [10], we simplify these expressions further and express the MCCRs in terms of the frequency response of the square-root Nyquist pulse shape.

A. Equivalent Discrete-Time Channel Model

Based on the Whittaker-Shannon-Kotel'nikov sampling theorem [11], [12], we can write $h(t)$ in (1) equivalently as

$$h(t) = \sum_{i=-\infty}^{\infty} h_i\phi(t - i\tau T_{\rm s}), \tag{8}$$

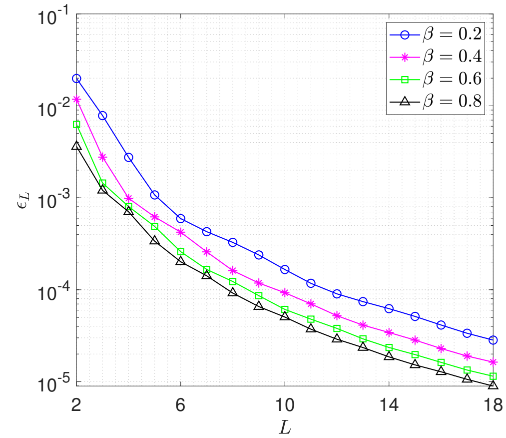

Fig. 1: ϵ_L versus L for SRRC pulses with different RoFs β.

where $\phi(t)$ is a $\tau T_{\rm s}$-orthonormal basis function such that

$$\int_{-\infty}^{\infty} \phi(t - i\tau T_{\rm s})\phi(t - k\tau T_{\rm s}){\rm d}t = \delta[i-k], \tag{9}$$

and

$$h_i \triangleq \int_{-\infty}^{\infty} h(t)\phi(t - i\tau T_{\rm s}){\rm d}t. \tag{10}$$

Here, $\delta[\cdot]$ denotes the Kronecker delta sequence. A condition for $\phi(t)$ is that its Fourier transform is constant over the bandwidth of $h(t)$ [12]. For capacity-achieving signaling, i.e., for $\tau = 1/(2BT_{\rm s})$, $\phi(t) = \frac{\sin(2\pi Bt)}{\pi t}$ meets this condition.

A sufficient statistic to estimate the transmitted sequence a_m, $m \in \{0, 1, \ldots, N-1\}$, based on $x(t)$ is given by

$$y_k = \int_{-\infty}^{+\infty} x(t)\phi(t - k\tau T_{\rm s}){\rm d}t = \sum_{m=0}^{N-1} a_m h_{k-m} + w_k, \tag{11}$$

where $k = \{-\infty, \ldots, \infty\}$, and $w_k \triangleq \int_{-\infty}^{+\infty} w(t)\phi(t - k\tau T_{\rm s}){\rm d}t$ is zero-mean discrete-time AWGN with variance $N_0/2$. Eq. (11) reveals that, in principle, an infinite number of $\tau T_{\rm s}$-spaced samples are needed to detect N symbols. This is due to the fact that the bandlimited pulses $h(t)$ cannot be time-limited. However, in practice, h_i decays quickly as $|i|$ increases. Hence, we may truncate h_i to length $2L+1$ and assume that $h_i = 0$ for $|i| > L$. The associated truncation error becomes negligible if the normalized energy, ϵ_L, contained in h_i, $|i| > L$, is negligible. ϵ_L is defined as follows

$$\epsilon_L = 1 - \frac{\sum_{i=-L}^{L}|h_i|^2}{\sum_{i=-\infty}^{+\infty}|h_i|^2} = 1 - \sum_{i=-L}^{L}|h_i|^2, \tag{12}$$

where we used the identity $\int_{-\infty}^{+\infty}|h(t)|^2{\rm d}t = \sum_{i=-\infty}^{+\infty}|h_i|^2 = 1$. Fig. 1 shows ϵ_L versus L for SRRC pulses with different roll-off factors (RoFs) β. As can be observed, ϵ_L decreases fast as L increases, where the rate of decrease increases with β.

In the following, we assume L is chosen sufficiently large for ϵ_L to be sufficiently small such that we can assume $h_i = 0$ for $|i| > L$. In this case, the sufficient statistics in (11) can be rewritten as follows

$$y_k = \sum_{m=0}^{N-1} a_m h_{k-m} + w_k, \qquad k = -L, \ldots, N+L-1, \tag{13}$$

i.e., we need $N + 2L$ $\tau T_{\rm s}$-spaced samples to detect the N symbols a_m, $m = 0, \ldots, N-1$. Thus, (13) can be equivalently rewritten in matrix form as follows

$$\mathbf{y} \triangleq \mathbf{H}\mathbf{a} + \mathbf{w}, \tag{14}$$

where $\mathbf{y} \triangleq [y_{-L}\ y_{-L+1}\ \ldots\ y_{N+L-1}]^T$, $\mathbf{a} \triangleq [a_0\ a_1 \ldots a_{N-1}]^T$, $\mathbf{w} \triangleq [w_{-L}\ w_{-L+1}\ \ldots\ w_{N+L-1}]^T$, and $(\cdot)^T$ denotes transposition. Furthermore, the $(N+2L)\times N$ convolution matrix $\mathbf{H}$ is given as follows

$$\mathbf{H} \triangleq \begin{bmatrix} h_{-L} & 0 & \cdots & 0 \\ h_{(-L+1)} & h_{-L} & \ddots & \vdots \\ \vdots & h_{(-L+1)} & \ddots & \vdots \\ h_L & \vdots & \ddots & h_{-L} \\ 0 & h_L & \ddots & h_{(-L+1)} \\ \vdots & \ddots & \ddots & \vdots \\ 0 & \cdots & 0 & h_L \end{bmatrix}. \tag{15}$$

Define now the singular value decomposition (SVD) of $\mathbf{H}$ as $\mathbf{H} = \mathbf{U}\boldsymbol{\Lambda}\mathbf{V}^T$, where $\mathbf{U}$ and $\mathbf{V}$ are orthogonal matrices and

$$\boldsymbol{\Lambda} \triangleq \left[\begin{array}{c|c} \begin{matrix} \lambda_0 & & 0 \\ & \ddots & \\ 0 & & \lambda_{N-1} \end{matrix} & 0_{N\times 2L} \\ \hline 0_{2L\times N} & 0_{2L\times 2L} \end{array}\right], \tag{16}$$

with the N non-zero singular values of $\mathbf{H}$ denoted by λ_m, $m \in \{0, 1, \ldots, N-1\}$. Without loss of optimality, we may precode the transmit symbol vector with $\mathbf{V}$, i.e., $\mathbf{a} \triangleq \mathbf{V}\tilde{\mathbf{a}}$, and filter the received signal with $\mathbf{U}^T$, i.e., $\tilde{\mathbf{y}} \triangleq \mathbf{U}^T\mathbf{y}$. Then, exploiting the orthogonality of $\mathbf{U}$ and $\mathbf{V}$, we obtain from (14)

$$\tilde{\mathbf{y}} = \boldsymbol{\Lambda}\tilde{\mathbf{a}} + \tilde{\mathbf{w}}, \tag{17}$$

where $\tilde{\mathbf{y}} \triangleq [\tilde{y}_0\ \tilde{y}_1\ \cdots\ \tilde{y}_{N+2L-1}]^T$, $\tilde{\mathbf{a}} \triangleq [\tilde{a}_0\ \tilde{a}_1\ \cdots\ \tilde{a}_{N-1}]^T$, and $\tilde{\mathbf{w}} = [\tilde{w}_0\ \tilde{w}_1\ \cdots\ \tilde{w}_{N+2L-1}]^T \triangleq \mathbf{U}^T\mathbf{w}$. Here, due to the orthogonality of $\mathbf{U}$, $\tilde{w}_k$ are i.i.d. AWGN samples with PSD $N_0/2$ similar to w_k. Hence, since the last $2L$ columns of $\boldsymbol{\Lambda}$ are zero, the continuous-time AWGN channel for FTN signaling in (1) can be equivalently modeled by N parallel discrete-time AWGN channels

$$\tilde{y}_m = \lambda_m\tilde{a}_m + \tilde{w}_m, \qquad m = 0, \ldots, N-1, \tag{18}$$

where $\mathbb{E}\{\tilde{a}_m^2\} = \tilde{p}_m$, $\sum_{m=0}^{N-1}\tilde{p}_m = N\sigma_{\mathrm{a}}^2$, and the SNR of the mth channel is $\gamma_m \triangleq 2\tilde{p}_m\lambda_m^2/N_0$.

B. MCCR: Parallel AWGN Channel Formulation

In the previous subsection, we have shown that assuming the pulse sequence h_i can be truncated to length $2L+1$, the transmission of N symbols at a rate of $1/(\tau T_{\mathrm{s}}) = 2B$ requires $N+2L$ channel uses and can be equivalently modeled in terms of a transmission over N parallel AWGN channels having SNRs γ_m, $m = 0, \ldots, N-1$.[2] Thus, the MCCR for the problem at hand, $R_{\mathrm{P}}(N,\epsilon)$ in [bits/s], can be obtained by exploiting the MCCR expression for parallel AWGN channels reported in [14, Fig. 1], where we set both the codeword length (denoted by n in [14]) and the number of parallel channels (denoted by K in [14]) equal to N, account for the fact that $N+2L$ samples are needed to detect N transmitted symbols, and take into account that the symbols are transmitted at a rate of $2B$ in FTN signaling. This leads to the following expression

$$R_{\mathrm{P}}(N,\epsilon) = \left(1 - \frac{1}{1+N/(2L)}\right)\left(C_{\mathrm{P}} - 2B\sqrt{\frac{V_{\mathrm{P}}}{N}}Q^{-1}(\epsilon) + \frac{B\log_2 N}{N}\right) + \mathcal{O}\left(\frac{1}{N}\right). \tag{19}$$

Here, C_{P} and V_{P} are the channel capacity in [bits/s] and dispersion of N parallel AWGN channels, respectively, and are given as follows

$$C_{\mathrm{P}} = \frac{B}{N}\sum_{m=0}^{N-1}\log_2\left(1 + \frac{2\tilde{p}_m\lambda_m^2}{N_0}\right), \tag{20}$$

and

$$V_{\mathrm{P}} = (\log_2 e)^2\frac{1}{2N}\sum_{m=0}^{N-1}\left(1 - \frac{1}{(1+\frac{2\tilde{p}_m\lambda_m^2}{N_0})^2}\right). \tag{21}$$

Eq. (20) and (21) are obtained by setting $K = N$ and SNR $\gamma_m = 2\lambda_m^2\tilde{p}_m/N_0$ (denoted by Ω_m in [14]) in the corresponding expressions for the capacity in [bits/s] and dispersion of parallel AWGN channels in [14, Fig. 1]. In this paper, for non-i.i.d. transmission, $\tilde{p}_m$, $m \in \{0, 1, \cdots, N-1\}$, we adopt water-filling power allocation[3]

$$\tilde{p}_m = \left[\Theta - \frac{N_0}{2\lambda_m^2}\right]^+, \tag{22}$$

where Θ is chosen such that $\sum_{m=0}^{N-1}\tilde{p}_m = N\sigma_{\mathrm{a}}^2$ holds. For equal power allocation, i.e., i.i.d. transmission, $\tilde{p}_m = \sigma_{\mathrm{a}}^2$.

C. MCCR Approximation

The non-zero diagonal entries of $\boldsymbol{\Lambda}^2$, i.e., $\lambda_0^2, \lambda_1^2, \ldots, \lambda_{N-1}^2$, are the eigenvalues of positive-definite (PD) matrix $\mathbf{H}^{\mathrm{T}}\mathbf{H} = \mathbf{V}\boldsymbol{\Lambda}^2\mathbf{V}^{\mathrm{T}}$. The eigenvalues of a PD matrix as its dimensions go to infinity can be obtained from Szegö's theorem.

Theorem 1. *(Szegö's theorem [10]): Let us denote the eigenvalues of the $M \times M$ PD Toeplitz matrix*

$$\mathbf{D} = \begin{bmatrix} d_0 & d_{-1} & \cdots & d_{1-M} \\ d_1 & d_0 & \cdots & d_{2-M} \\ \vdots & \ddots & \ddots & \vdots \\ d_{M-1} & \cdots & d_1 & d_0 \end{bmatrix} \tag{23}$$

as $\eta_0, \eta_1, \cdots, \eta_{M-1}$. Then, for an arbitrary continuous function $g(\cdot)$, the following identity holds:

$$\lim_{M\to\infty}\frac{1}{M}\sum_{m=0}^{M-1}g(\eta_m) = \int_{-\frac{1}{2}}^{\frac{1}{2}}g(\tilde{D}(F))\,\mathrm{d}F, \tag{24}$$

where $\tilde{D}(F) = \sum_{m=-\infty}^{\infty}d_m e^{-j2\pi Fm}$ is the discrete-time Fourier transform (DTFT) of $\{\cdots\ d_{-2}\ d_{-1}\ d_0\ d_1\ d_2\ \cdots\}$.

Matrix $\mathbf{H}^{\mathrm{T}}\mathbf{H}$ has the form of matrix $\mathbf{D}$ in (23) with $M = N$ and $d_k = \sum_{m=-L}^{L}h_m h_{k-m}$, $k \in \{-2L, \cdots, 2L\}$, and $d_k = 0$ otherwise. Furthermore, the DTFT of d_k is given by $\tilde{D}(F) = \sum_{m=-\infty}^{\infty}d_m e^{-j2\pi Fm} = |\tilde{H}(F)|^2$ with $\tilde{H}(F) = \sum_{m=-L}^{L}h_m e^{-j2\pi Fm}$. In addition, exploiting (8), the properties of $\phi(t)$, $1/(\tau T_{\mathrm{s}}) = 2B$, and assuming L is chosen sufficiently large such that truncation error ϵ_L is negligible, we

[2]Note that infinite blocklength FTN signaling has also been modeled in terms of parallel AWGN channels in [13].

[3]We note that the water-filling power allocation is suboptimal for finite N, but becomes asymptotically optimal as $N \to \infty$.

obtain $H(f) = \frac{1}{\sqrt{2B}}\tilde{H}(F)$ with $f = 2BF$. Hence, taking into account $H^*(f) = H(-f)$, (24) can be rewritten as follows

$$\lim_{N\to\infty} \frac{1}{N}\sum_{m=0}^{N-1} g(\lambda_m^2) = \frac{1}{B}\int_0^B g\left(2B|H(f)|^2\right)\,\mathrm{d}f. \quad (25)$$

Exploiting this asymptotic identity, we provide an approximate expression for the MCCR for FTN signaling.

Proposition 1. *For sufficiently large N and L, the maximum channel coding rate for FTN signaling, $R_{\mathrm{P}}^{\mathrm{NIID}}(N,\epsilon)$ in [bits/s], can be approximated by*

$$R_{\mathrm{FTN}}^{\mathrm{NIID}}(N,\epsilon) = \left(C_{\mathrm{FTN}}^{\mathrm{NIID}} - 2B\sqrt{\frac{V_{\mathrm{FTN}}^{\mathrm{NIID}}}{N}}Q^{-1}(\epsilon) + \frac{B\log_2 N}{N}\right) \times \left(1 - \frac{1}{1+N/(2L)}\right) + \mathcal{O}\left(\frac{1}{N}\right) + \mathcal{O}\left(\frac{1}{L^{\alpha}}\right), \quad (26)$$

where $C_{\mathrm{FTN}}^{\mathrm{NIID}}$ and the optimal power allocation $p(f)$ are given by (4) and (5), respectively, the value of the positive parameter α depends on the pulse shape, and

$$V_{\mathrm{FTN}}^{\mathrm{NIID}} = \frac{(\log_2 e)^2}{2B}\int_0^B \left(1 - \frac{1}{\left(1 + \frac{4Bp(f)|H(f)|^2}{N_0}\right)^2}\right)\mathrm{d}f. \quad (27)$$

The MCCR for FTN signaling with i.i.d. symbols, $R_{\mathrm{P}}^{\mathrm{IID}}(N,\epsilon)$, can be approximated by

$$R_{\mathrm{FTN}}^{\mathrm{IID}}(N,\epsilon) = \left(C_{\mathrm{FTN}}^{\mathrm{IID}} - 2B\sqrt{\frac{V_{\mathrm{FTN}}^{\mathrm{IID}}}{N}}Q^{-1}(\epsilon) + \frac{B\log_2 N}{N}\right) \times \left(1 - \frac{1}{1+N/(2L)}\right) + \mathcal{O}\left(\frac{1}{N}\right) + \mathcal{O}\left(\frac{1}{L^{\alpha}}\right), \quad (28)$$

where $V_{\mathrm{FTN}}^{\mathrm{IID}}$ is obtained from $V_{\mathrm{FTN}}^{\mathrm{NIID}}$ for $p(f) = P_{\mathrm{s}}/(2B)$.

Proof: $R_{\mathrm{FTN}}^{\mathrm{NIID}}(N,\epsilon)$ is obtained from $R_{\mathrm{P}}(N,\epsilon)$ by applying (25) to C_{P} and V_{P} in (20) and (21), respectively, and truncating the sum on the left-hand side of (25) to a finite number of terms. Thereby, we have $g(x) = B\log_2(1 + 2[\Theta - N_0/(2x)]^+ x/N_0)$ and $g(x) = (\log_2 e)^2(1 - 1/(1 + 2[\Theta - N_0/(2x)]^+ x/N_0)/2$ for C_{P} and V_{P}, respectively. The term $\mathcal{O}\left(\frac{1}{L^{\alpha}}\right)$ indicates the order of the approximation error in terms of L which vanishes for $L \to \infty$. The result for i.i.d. signaling is obtained by uniformly allocating the available power P over the entire bandwidth of $2B$. □

Remark 1: Based on (25), the approximations in Proposition 1 become asymptotically tight for $L \to \infty$ and $N \to \infty$. For finite L and N, the accuracy of the approximation can be evaluated numerically. To this end, we define the relative approximation error incurred by Szego's theorem in (25) for finite L and N as follows

$$E \triangleq \frac{\left|\frac{1}{N}\sum_{m=0}^{N-1} g(\lambda_m^2) - \frac{1}{B}\int_0^B g\left(2B|H(f)|^2\right)\mathrm{d}f\right|}{\frac{1}{N}\sum_{m=0}^{N-1} g(\lambda_m^2)}. \quad (29)$$

Fig. 2 shows E for capacity $C_{\mathrm{FTN}}^{\mathrm{NIID}}$ and dispersion $V_{\mathrm{FTN}}^{\mathrm{NIID}}$ for an SRRC pulse with $\beta = 0.8$ and SNR $\gamma \triangleq 10\log_{10}(P/(N_0 W))$ [dB], where $g(\cdot)$ in (29) was replaced with the appropriate function specified in the proof of Proposition 1. As can be observed, for sufficiently large L ($L = 45$ in this case), E decays as $1/N$ for both $C_{\mathrm{FTN}}^{\mathrm{NIID}}$ and $V_{\mathrm{FTN}}^{\mathrm{NIID}}$. For smaller L, E decays more slowly. Nevertheless, our results in Fig. 4 will show that $R_{\mathrm{FTN}}^{\mathrm{NIID}}(N,\epsilon)$ closely approximates $R_{\mathrm{P}}^{\mathrm{NIID}}(N,\epsilon)$ even for values of L as small as 4. This is due to the fact that although, for small L, E decays slowly as N increases, the absolute value of E, which determines the quality of the approximation of $R_{\mathrm{P}}^{\mathrm{NIID}}(N,\epsilon)$ in terms of $R_{\mathrm{FTN}}^{\mathrm{NIID}}(N,\epsilon)$, is still small compared to the value of $R_{\mathrm{FTN}}^{\mathrm{NIID}}(N,\epsilon)$.

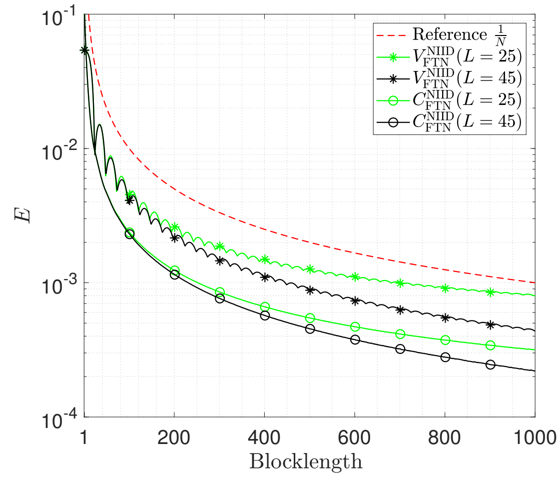

Fig. 2: Relative approximation error E versus blocklength, N, for $C_{\mathrm{FTN}}^{\mathrm{NIID}}$ and $V_{\mathrm{FTN}}^{\mathrm{NIID}}$ for an SRRC pulse with $\beta = 0.8$ and $\gamma = 20$ dB.

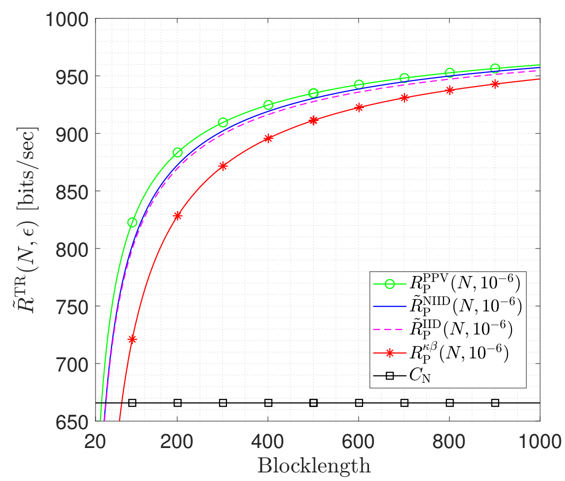

Fig. 3: Normal approximation with the third-order term of MCCR and corresponding achievability and converse bounds versus blocklength, N, for SRRC pulse with $\beta = 0.7$, $L = 4$, and $\gamma = 20$ dB.

Remark 2: The term $(1 - (1 + N/(2L))^{-1})$ in (26) and (28) accounts for the rate loss caused by the fact that $N + 2L$ samples are required to detect N transmitted symbols in FTN signaling. This term approaches unity for $N/(2L) \gg 1$. The remaining terms in (26) and (28) are similar to those present in the MCCR expressions for other types of channels [6]. In the limit as $N \to \infty$ and $\epsilon \to 0$, $R_{\mathrm{FTN}}^{\mathrm{NIID}}(N,\epsilon)$ and $R_{\mathrm{FTN}}^{\mathrm{IID}}(N,\epsilon)$ converge to the respective capacity expressions $C_{\mathrm{FTN}}^{\mathrm{NIID}}$ and $C_{\mathrm{FTN}}^{\mathrm{IID}}$. The speed of convergence is investigated in the next section.

IV. Numerical Evaluation

For our simulations, we consider the normal approximation including the third-order term (i.e., $B\log_2 N/N$) of $R_{\mathrm{FTN}}^{\mathrm{NIID}}(N,\epsilon)$ and $R_{\mathrm{FTN}}^{\mathrm{IID}}(N,\epsilon)$, which is defined as follows

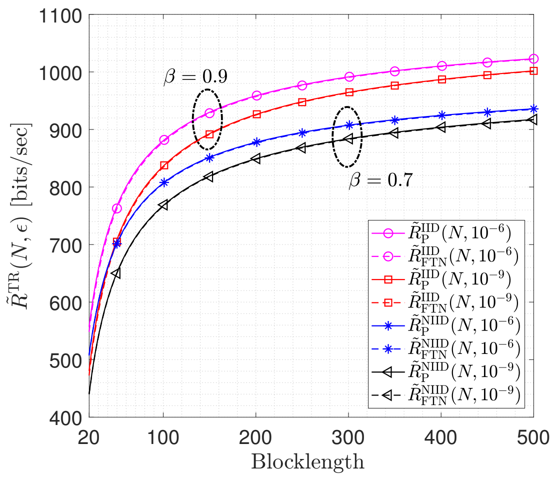

Fig. 4: Normal approximation of MCCR versus blocklength for SRRC pulses with RoF β, $L = 4$, and $\gamma = 20$ dB.

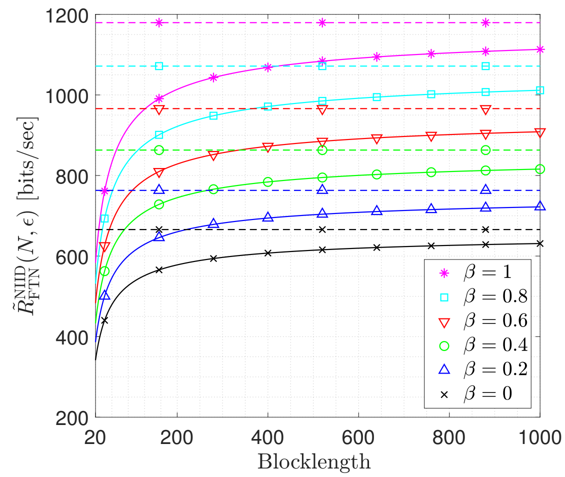

Fig. 5: Normal approximation of MCCR versus blocklength for water -filling power allocation with $\epsilon = 10^{-6}$, $L = 4$, and $\gamma = 20$ dB.

$$\tilde{R}_{\mathrm{FTN}}^{\mathrm{TR}}(N,\epsilon) = \left(1 - \frac{1}{1 + N/(2L)}\right) \times \left(C_{\mathrm{FTN}}^{\mathrm{TR}} - 2B\sqrt{\frac{V_{\mathrm{FTN}}^{\mathrm{TR}}}{N}}Q^{-1}(\epsilon) + \frac{B\log_2 N}{N}\right) \quad \text{[bits/s]}, \tag{30}$$

where $\mathrm{TR} \in \{\mathrm{NIID}, \mathrm{IID}\}$. We used SRRC pulses, $W = 100$ Hz, and $L = 4$. For $L = 4$, the approximation error ϵ_L in (12) is below 10^{-2} for all considered values of β in Fig. 1.

In Fig. 3, we compare the derived normal approximation with the $\kappa\beta$ achievability bound, $R_{\mathrm{P}}^{\kappa\beta}(N,\epsilon)$, and Polyanskyi-Poor-Verdu (PPV) meta-converse bound, $R_{\mathrm{P}}^{\mathrm{PPV}}(N,\epsilon)$ [4] for FTN signaling. These bounds are obtained by using the $\kappa\beta$ achievability bound in [15] and the PPV meta-converse bound in [14] for parallel AWGN channels. Fig. 3 suggests that the normal approximation accurately characterizes the theoretical MCCR for sufficiently large blocklengths where the PPV upper bound and the $\kappa\beta$ lower bound approach each other.

Fig. 4 compares the normal approximation of $R_{\mathrm{FTN}}^{\mathrm{TR}}(N,\epsilon)$ derived in Proposition 1 with the normal approximation of $R_{\mathrm{P}}(N,\epsilon)$ in (19) for different RoFs β and different MBEP ϵ. The normal approximation of $R_{\mathrm{P}}(N,\epsilon)$ is obtained by dropping the term $\mathcal{O}(1/N)$ in (19) and denoted by $\tilde{R}_{\mathrm{P}}^{\mathrm{NIID}}(N,\epsilon)$ and $\tilde{R}_{\mathrm{P}}^{\mathrm{IID}}(N,\epsilon)$ for water-filling and equal power allocation, respectively. As can be observed, for all considered values of β, ϵ, and $N > 20$, $\tilde{R}_{\mathrm{FTN}}^{\mathrm{TR}}(N,\epsilon)$ closely approximates $\tilde{R}_{\mathrm{P}}^{\mathrm{TR}}(N,\epsilon)$ for both water-filling and equal power allocation.

Fig. 5 compares the MCCR of FTN signaling with finite and infinite blocklength coding for water-filling power allocation and SRRC pulses with different RoFs β. As expected, $\tilde{R}_{\mathrm{FTN}}^{\mathrm{NIID}}(N,\epsilon)$ increases with β because FTN signaling can exploit the higher excess bandwidth. Note that the curves for $\beta = 0$ correspond to the case of Nyquist signaling. For a given blocklength N, the gap between the MCCRs for finite and infinite blocklength coding increases with β. Considering (30) this implies that the square root of $V_{\mathrm{FTN}}^{\mathrm{NIID}}$ grows faster with β than capacity for infinite blocklength coding, $C_{\mathrm{FTN}}^{\mathrm{NIID}}$.

V. Conclusion

In this letter, we derived an easy-to-evaluate approximation for the MCCR for finite blocklength FTN signaling. We showed that the MCCR for finite blocklength FTN signaling exceeds the Shannon capacity for infinite blocklength Nyquist signaling. Hence, FTN signaling is an effective means to mitigate the rate penalty incurred by finite blocklength transmission. This property makes FTN signaling a promising candidate for short-packet transmission supporting URLLC use cases. The derived analytical expression for the MCCR can be exploited for protocol design and resource allocation.

References

[1] P. Popovski, J. J. Nielsen, C. Stefanovic, E. De Carvalho, E. Strom, K. F. Trillingsgaard, A.-S. Bana, D. M. Kim, R. Kotaba, and J. Park, “Wireless access for ultra-reliable low-latency communication: Principles and building blocks,” *IEEE Network*, vol. 32, no. 2, pp. 16–23, Apr. 2018.

[2] J. E. Mazo, “Faster-than-Nyquist signaling,” *The Bell System Technical Journal*, vol. 54, no. 8, pp. 1451–1462, Oct. 1975.

[3] J. B. Anderson, F. Rusek, and V. Öwall, “Faster-than-Nyquist signaling,” *Proc. IEEE*, vol. 101, no. 8, pp. 1817–1830, Aug. 2013.

[4] Y. Polyanskiy, H. V. Poor, and S. Verdú, “Channel coding rate in the finite blocklength regime,” *IEEE Trans. Inf. Theory*, vol. 56, no. 5, pp. 2307–2359, May 2010.

[5] W. Yang, G. Durisi, T. Koch, and Y. Polyanskiy, “Quasi-static multiple-antenna fading channels at finite blocklength,” *IEEE Trans. Inf. Theory*, vol. 60, no. 7, pp. 4232–4265, Jul. 2014.

[6] V. Y. F. Tan and M. Tomamichel, “The third-order term in the normal approximation for the AWGN channel,” *IEEE Trans. Inf. Theory*, vol. 61, no. 5, pp. 2430–2438, May 2015.

[7] G. Durisi, T. Koch, J. Östman, Y. Polyanskiy, and W. Yang, “Short-packet communications over multiple-antenna Rayleigh-fading channels,” *IEEE Commun. Lett.*, vol. 64, no. 2, pp. 618–629, Feb. 2015.

[8] T. M. Cover and J. A. Thomas, *Elements of Information Theory*, 2nd ed. John Wiley & Sons, 2012.

[9] S. Shama, L. Ozarow, and A. D. Wyner, “Information rates for a discrete-time Gaussian channel with intersymbol interference and stationary inputs,” *IEEE Trans. Inf. Theory*, vol. 37, no. 6, pp. 1527–1539, Nov. 1991.

[10] R. M. Gray, “Toeplitz and circulant matrices: A review,” *Foundations and Trends in Communications and Information Theory*, vol. 2, no. 3, pp. 155–239, 2006.

[11] A. Zayed, *Advances in Shannon’s Sampling Theory*. Routledge, 2018.

[12] A. Prlja and J. B. Anderson, “Reduced-complexity receivers for strongly narrowband intersymbol interference introduced by faster-than-Nyquist signaling,” *IEEE Trans. Commun.*, vol. 60, no. 9, pp. 2591–2601, Sept. 2012.

[13] Y. J. D. Kim, “Properties of faster-than-Nyquist channel matrices and folded-spectrum, and their applications,” in *Proc. IEEE WCNC*, Doha, Qatar, Apr. 2016.

[14] T. Erseghe, “Coding in the finite-blocklength regime: Bounds based on Laplace integrals and their asymptotic approximations,” *IEEE Trans. Inf. Theory*, vol. 62, no. 12, pp. 6854–6883, Dec. 2016.

[15] J.-H. Park and D.-J. Park, “A new power allocation method for parallel AWGN channels in the finite block length regime,” *IEEE Wireless Commun. Lett.*, vol. 16, no. 9, pp. 1392–1395, Sept. 2012.